Journal of Mechanical Engineering Research and Developments
ISSN: 1024-1752
CODEN: JERDFO
Vol. 43, No. 7, pp. 100-108
Published Year 2020

Numerical Investigation of Turbulent Air Flow Convective Heat Transfer through a Trapezoidal Duct

Salah Sabeeh Abed AlKareem[†], Ahmed Fakhrey Khudheyer[‡], Faiz F. Mustafa[‡]

[†] Automated Manufacturing Engineering Depart., College of Engineering, University of Baghdad/Al–Khwarizmi.
[‡] Mechanical Engineering Department, College of Engineering, University of Al-Nahrain, Baghdad- Iraq.

*Corresponding Author Email: dr.salah1961@coagri.uobaghdad.edu.iq ; Drahmed955@eng.nahrainuniv.edu.iq ; dr.faiz@kecbu.uobaghdad.edu.iq

ABSTRACT: Airflow through a circular and noncircular duct has several applications in life such as the air-conditioning system, electronic devices, and food industrials. The efficiency depends greatly upon channel's cross-section and liquid media. This study has performed to investigate the effect of the geometrical duct and boundary conditions for turbulent airflow and heat transfer characteristics. Several cases have investigated to discover the impact of the heating side on the Nusselt number and friction factor, by utilizing the construction of computer engineering mathematical models and taking into account the analysis of the results of different forms of heating lower, upper, and both sides. The properties of heat transfer have analyzed for the conditions of turbulent flow using ANSYS Fluent2019R1 in which the turbulence model of trapezoidal-shaped with a constant thermal discharge (8000 W / m²) and airflow velocity of 2.5 m / sec have investigated. An enhancement of heat transfer characteristics have clarified in which three cases were tested and compared for Reynolds number of 4200. Results showed the average Nusselt number and friction factor significantly affected by the Reynolds number and the shape of the duct if compared with other studies mentioned in the previous works.

KEYWORDS: Air Flow, Turbulent Flow, Convection Heat Transfer, Trapezoidal Duct, ANSYS Fluent.

INTRODUCTION

Studies of the fluid flow with arbitrarily duct have investigated extensively due to its importance in different engineering applications. Consequently, various researches have performed to estimate the convective heat transfer and fluid flow characteristics in heat exchangers design, solar air heat, and refrigeration. Duct with arbitrary shaped has described as a non-circular pipe [1]. Behavior of heat transfer and pressure drop of the dual/quadruple twisted tapes in square ducts has investigated and studied using different configurations such as numerical simulations, flow structure and thermo-hydraulic characteristics. Analysis have conducted using the RNG k-ε turbulent model based on uniform wall heat flux condition with Reynolds numbers from 6000 to 14000. Thermo-hydraulic characteristics depend on the number and configuration of tapes in which tape number is proportional to the heat transfer rate [2].

Several experiments were performed at a rate of 2.5 twist ratio based on the provision of constant heat flux. Regularly spaced quadruple twisted tapes have a heat transfer rate of up to 6.6 per cent above that of quadruple twisted tapes and a overall thermal enhancement factor of 1.27 [3]. A Pentagonal rib which fixed at the bottom of the rectangular heated wall channel have utilized in which the effect of heat transfer that related with multi-channel twisted tapes, under uniform flux condition have scrutinized based on Reynolds number from 800 to 15000. It showed that the thermal performance factor reaches its maximum value of 1.04 at 5000 Reynolds [4].

Different experiments have employed to find the friction factor and the enhancement of Heat transfer using various Reynolds numbers (9400 - 58850), (6 – 12) pitch to height ratio, and (0 – 20) chamfering angles. A reliable improvement for Pentagonal ribs have recorded especially at high Reynolds numbers. The cross-section of ducts categorized as orthogonal and non- orthogonal ducts (such as trapezoidal), in which the generated own are extremely

complex [5]. Furthermore, the influence of the swirl, impinging jets, and effusion flow has experimentally studied. An enlarged model of the trapezoidal duct has built up in the nearby region the leading-edge of the blade. It showed that the large jets have a reliable contribution in inducing and impelling strong anticlockwise vortex. The hydraulic diameter have utilized instead of the original diameter of the circular tube for Reynolds number calculation, which has used to estimate friction factor and Nu from the correlations. In non-circular duct, friction factor and heat transfer coefficient have estimated based on the hydraulic diameter of the noncircular duct as stated in [6].

Ducts with trapezoidal cross-sections appear considerably in the compact regenerative heat exchangers, recuperative heat exchangers, and other cooling systems. Fully developed flow and thermal fields for laminar conditions have investigated extensively, however the developed hydrodynamic and thermal fields have practiced in the entrance region only [7]. At turbulent conditions, fully developed velocity distributions and secondary flow patterns have measured for a specific duct as stated in [8].

Moreover, another experimental study conducted as, for a trapezoidal duct with the corner angle 75^{o} [9]. It suggested that the friction factor could be calculated by the well-known Blasius formula if the hydraulic diameter have used. Heat transfer and fluid flow characteristics investigated numerically using the CFD technique for water flow, through an annulus of a tube equipped with the interior trapezoidal grooves. Tests have performed for $5000 \leq Re \leq 13500$ in which results have shown an increasing of Nusselt number with 43% of its nominal value, and thermal-hydraulic performance also have enhanced with 40% from its nominal value for trapezoidal grooved tube compared with that for plane tube as stated [10].

Numerical investigation for 3D wedge-shaped ribs square duct for a Reynolds number range 10000 to 30000 have conducted in which Iso flux has applied on one side surface of the duct. k-ϵ turbulence model used to assess the present case. Both heat transfer and friction factor have estimated. The objective of the present article is obtaining the effect of the (geometry and heated side) for turbulent airflow on the characteristics of heat transfer, fluid flow with Nusselt number and friction factor through a trapezoidal duct cross-sectional area.

MATHEMATICAL MODELING

Problem Description

A straight duct (symmetry conditions) with a trapezoidal cross-section and specification of 2 mm thickness have considered as shown in Figure 1. The upper side length of the cross-section is 20 mm and the duct length is L = 200 mm. fully developed turbulent flow and periodic conditions at the inlet and outlet have imposed. The ratio of the height (30 mm) to the upper side length has defined as a, (a= 30/20 = 1.5). The overall performance of the duct in terms of the friction factor and Nusselt number have determined numerically. The secondary flow motion in the cross-sectional plane has also a major concern. The turbulence model has used as described in the following sections.

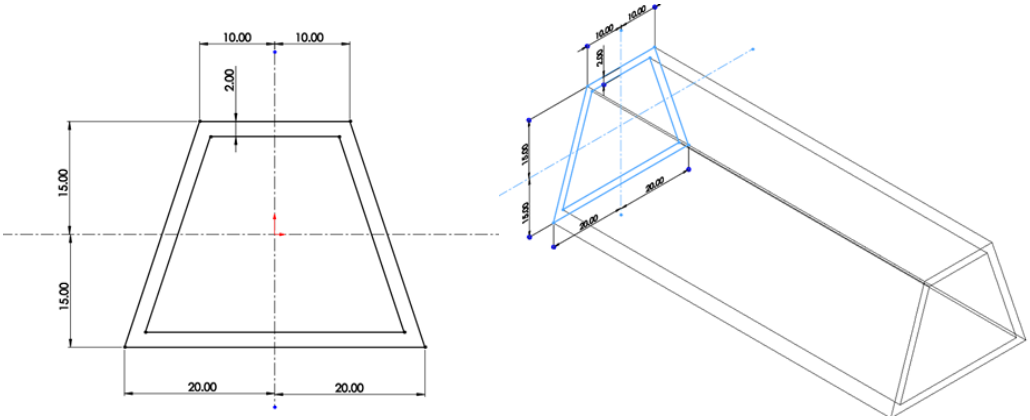

Front view Isometric view

Figure 1. Scheme for a studied duct with 200mm of length. (All dimensions in mm)

Model Assumption

The following assumptions have considered depending on the above duct configuration Figure 1:

1. Fluid flow is incompressible.
2. Three -dimensional turbulent airflow through the trapezoidal duct.
3. Steady-State conditions with fully developed.
4. Neglecting the convection in the x, y-direction.
5. Assuming the Inlet velocity is (2.5 m/s), and constant heat flux of (8000watt/m²).

Governing Equations

The following conservation equations related to the x, y, and z directions can be written as follows [7]:

$$\frac{\partial V}{\partial y}+\frac{\partial W}{\partial z}=0 \tag{1}$$

$$\frac{\partial}{\partial y}(VU)+\frac{\partial}{\partial z}(WU)=D_n-\frac{\partial \underline{uv}}{\partial y}-\frac{\partial \underline{uw}}{\partial z}+\frac{1}{Re}\left(\frac{\partial^2 U}{\partial y^2}+\frac{\partial^2 U}{\partial z^2}\right) \tag{2}$$

$$\frac{\partial}{\partial y}(VV)+\frac{\partial}{\partial z}(WV)=-\frac{\partial P}{\partial y}-\frac{\partial \underline{v^{\rightarrow 2}}}{\partial y}-\frac{\partial vW}{\partial z}+\frac{1}{Re}\left(\frac{\partial^2 V}{\partial y^2}+\frac{\partial^2 V}{\partial z^2}\right) \tag{3}$$

$$\frac{\partial}{\partial y}(VW)+\frac{\partial}{\partial z}(WW)=-\frac{\partial P}{\partial z}-\frac{\partial vw}{\partial y}-\frac{\partial w^2}{\partial z}+\frac{1}{Re}\left(\frac{\partial^2 W}{\partial y^2}+\frac{\partial^2 W}{\partial z^2}\right) \tag{4}$$

$$\frac{\partial}{\partial y}(Vk)+\frac{\partial}{\partial z}(Wk)=\frac{1}{Re}\frac{\partial}{\partial y}\left[\left(\frac{v_t}{\sigma_k}+1\right)\frac{\partial k}{\partial y}\right]+\frac{1}{Re}\frac{\partial}{\partial z}\left[\left(\frac{v_t}{\sigma_k}+1\right)\frac{\partial k}{\partial z}\right]+P-\varepsilon \tag{5}$$

$$\frac{\partial}{\partial y}(V\varepsilon)+\frac{\partial}{\partial z}(W\varepsilon)=\frac{1}{Re}\frac{\partial}{\partial y}\left[\left(\frac{v_t}{\sigma_\varepsilon}+1\right)\frac{\partial \varepsilon}{\partial y}\right]+\frac{1}{Re}\frac{\partial}{\partial z}\left[\left(\frac{v_t}{\sigma_\varepsilon}+1\right)\frac{\partial \varepsilon}{\partial z}\right]+C_{e1}\frac{P}{k}\varepsilon-C_{e2}\frac{\varepsilon^2}{k} \tag{6}$$

$$v_t=C_\mu Re\ \frac{k^2}{\varepsilon} \tag{7}$$

$$\underline{uv}=\frac{-v_t}{Re}\frac{\partial U}{\partial y}, \underline{uw^{\rightarrow}}=-\frac{v_t}{Re}\frac{\partial U}{\partial z} \tag{8}$$

$$\underline{v}^2=\frac{2}{3}k-4C_\mu\frac{v_t k}{\varepsilon}\left[\left(\frac{C_D}{12}+\frac{C_E}{3}\right)\left(\frac{\partial U}{\partial y}\right)^2+\left(-\frac{C_D}{6}+\frac{C_E}{3}\right)\left(\frac{\partial U}{\partial z}\right)^2\right]-2\frac{v_t}{Re}\frac{\partial V}{\partial y} \tag{9}$$

$$\underline{w^2}=\frac{2}{3}k-4C_\mu\frac{v_t k}{\varepsilon}\left[\left(-\frac{C_D}{6}+\frac{C_E}{3}\right)\left(\frac{\partial U}{\partial y}\right)^2+\left(-\frac{C_D}{12}+\frac{C_E}{3}\right)\left(\frac{\partial U}{\partial z}\right)^2\right]-2\frac{v_t}{Re}\frac{\partial W}{\partial y} \tag{10}$$

$$\underline{vW}=-C_\mu C_D\frac{v_t k}{Re\varepsilon}\frac{\partial U}{\partial y}\frac{\partial U}{\partial z}-\frac{v_t}{Re}\left(\frac{\partial V}{\partial z}+\frac{\partial W}{\partial y}\right) \tag{11}$$

$$P=\frac{v_t}{Re}\left[\left(\frac{\partial U}{\partial y}\right)^2+\left(\frac{\partial U}{\partial z}\right)^2\right] \tag{12}$$

The following constants are based in the calculations, $C_\mu=0.09, C_{\varepsilon 1}=1.44, C_{e2}=1.92, \sigma_k=\sigma_\varepsilon=1.225$.

Walls Boundary Conditions

1- For all cases velocity at:

z = 0:	w = 2.5 m/sec; P = Patm; u = 0, v = 0
y = 0:	U, v, w = 0
y = 30 mm:	u = v = w =0
the left and right walls:	u = v = w = 0

2- Heat flux at:

Bottom heated side (at y = 0; q = 8000 w/m²) and (at y= 30 mm; left side and right sides; q = 0, other sides are insulated).

top side heated (y= 30 mm; q=8000 w/m²; other sides are insulated).

top and bottom sides are heated (y= 0, y= 30 mm, q=8000 w/m², other sides are insulated).

Theoretical Calculations

Fully developed Nusselt number for a smooth duct, Dittus-Boelter [3]:

$Nu = 0.023Re^{0.8}Pr^{n}$, n= 0.4, for heating fluid flow. (13)

Average Nusselt number calculated from:

$Nu_{Avg} = \frac{h_{Avg} \times D_h}{k_{air}}$, Dh =0.08m duct hydraulic diameter. (14)

Average heat transfer coefficient calculated from:

$h_{Avg} = \frac{q}{(T_{S_{Avg}} - T_{Air_{Bulk}})}$(W/m².°C) (15)

Mean Velocity (V) using the Reynolds number considered obtained from the next Equation.

Re=ρVDh/μ, (16)

Nusselt number and friction factor are obtained using the following equations

Nu=hDi/k, h=((Q/A)/(Tw-Tb)) (17)

Tb = (Ti+T0)/2, f= ((ΔP) / (L/D) ρV2/2) (18)

The following equation is used to find enhancement efficiency:

Friction factor ratio = (Nu/Nu0) / (f/fo) 1/3 (19)

Dittus-Boelter results related to Nusselt number and friction factor related to (6000-14000) Reynold,s number is tabulated below, see Table 1.

Nusselt number: Nu=0.023 $Re^{0.8}$. $Pr^{0.4}$ for 6000 ≤ Re ≤ 42000 (20)

Friction Factor: f = 0.4161Z-0.279 for 6000 ≤ Re ≤ 42000 (21)

Table 1. Theoretical Parameters Calculations

S. No	Mass flow rate	Re	f	Nu
1	0.003334	7757.98	0.0338	25.79
2	0.004108	9557.67	0.0316	30.48
3	0.00474	11028.08	0.0303	34.17
4	0.005304	12341.18	0.0295	37.39

NUMERICAL ANALYSIS

Numerical analysis has carried out using the finite volume method and the upwind schematic to unravel the discretization equations, 3D turbulent steady flow has utilized. The numerical analysis has achieved using the F.D.M. and described the governing equations with above boundary conditions and assumptions. It solved by the upwind schematic and simulated using commercial Package Fluent Ansys2019R1, in which the properties of the working fluid (air) varied with temperatures.

The air thermal conductivity can be fined as:

$$k_{air} = 1.5207E\text{-}11*T^3 - 4.8574E\text{-}08*T^2 + 1.0184E\text{-}04*T - 3.9333E\text{-}04 \quad (22)$$

the air density is $\rho_{air} = 360.77819*T - 1.00336$ (23)

the kinematic viscosity of air as:

$$\mu_{air} = -1.1555E\text{-}14*T^3 + 9.5728E\text{-}11*T^2 + 3.7604E\text{-}08*T - 3.4484E\text{-}06 \quad (24)$$

and the specific heat for Air as:

$$C_{pair} = 1.9327E - 10 * T^4 - 7.9999E - 07*T^3 + 1.1407E - 03*T^2 - 4.4890E - 01*T + 1.0575E + 03 \quad (25)$$

Table 2 represents the properties of fluid flow (air) and duct material (Aluminum) for the programmed equations.

Table 2. Air and Material Properties

Properties at 1atm	Fluid (Air)	Aluminum
Density(kg/m3)	1.156	2670
Specific heat(J/kg.k)	1005	860
Thermal conductivity(W/mK)	0.027	140
Prandtl number	0.7	-
Kinematic viscosity(m2/sec)	16.5x10 ¯6	-

Mesh Generation

First of all, researchers have selected several number and sizes of elements until reaching stability of the selection for the number of elements and size. Then, a hexagonal mesh element for the computational domain have selected with a number and size of elements are 23422072 and 10-9 respectively to acquire high accurate results as represented in Figure 2.

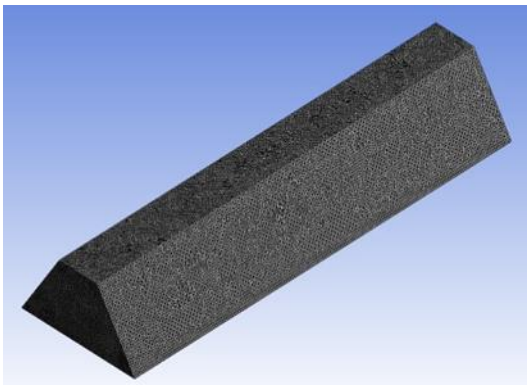

Figure 2. Mesh generation.

Mesh Independency

The numbers of nodes and the simulation time for the three cases have simulated using the standard k-ε model which highlighted in Table 3.

Table 3. Mesh Independence.

Mesh Resolution	Coarse Mesh(M1)	Medium mesh(M2)	Fine mesh (M3)
Number of nodes	79859	151740	23422072
CFD simulation time	1hrs 10mins	2hrs 16mins	7hrs 05mins
Estimated f	0.03215	0.04133	0.04214

RESULTS AND DISCUSSION

For the same range of temperature difference from Tmin =300K to Tmax = 520K, and for the same boundary conditions, it can be shown that the temperature distribution different from positions to another according to the distance along the x-direction from the inlet section. The temperature distribution showed in Fig. 3 which represents the three states of duct heating: the upper duct heating, the lower duct heating, and both sides duct heating. Heating process for both sides is higher if compared with the other lower, and upper side, because the heating process takes place for the fluid (air) that runs along the trapezoidal duct deviated from two directions. The air will receive heat from two directions that lead to increase temperatures in the direction of flow, as shown in Fig. 3c. It has noted that the flow lines of temperature concentrate heavily in the upper and lower sides. This will lead that the receding of these lines in the center of the stream at multiple sections along the duct from the entrance and exit at (5mm, 20mm, 40mm, 80mm, 120mm, 160mm, 175mm, and 199mm), the temperature distribution during the duct has shown in Fig. 3a and Fig. 3b.

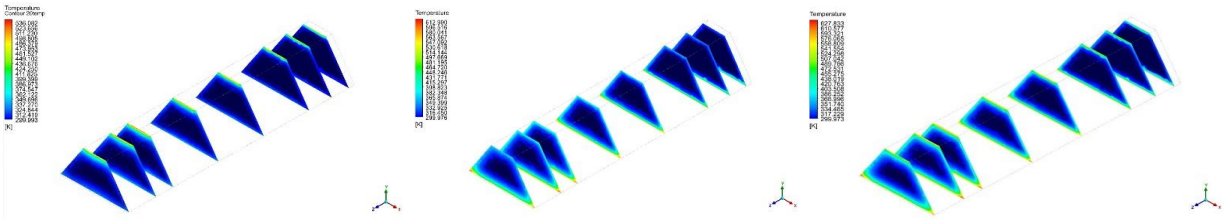

Figure 3. Temperature contour of the heating duct (a) upper (b) lower and (c) both sides.

Differences have noticed in the distribution of temperatures across each section and for each case to the direct impact on the thickness of the congested thermal boundary layer that depends directly on the Prandtls number, temperatures and the other hydraulic boundary layer, which depends directly on the changing of Reynolds number under-speed effect. This is confirmed by the velocity distribution at the length of duct, represented in Figure 4.

Figure 4. Velocity contours along the length of the duct (a) upper, (b) lower, and (c) both sides heated.

The temperature distributions for heating air, as shown in Fig. 5 represents instability of air temperature along the stream. Instability of air temperature increases as a result of heating for the three aforementioned cases. Air temperature with the process of direct heating for both sides have a higher value if compared with the previous two cases as represented in Fig. 6, which shows the distribution of temperatures for each heated surface. As a result of the rise in temperature in the heated surfaces and the air flows inside the stream leads to decrease in the difference between the surface temperature and the air temperature at the same cross-section of the stream.

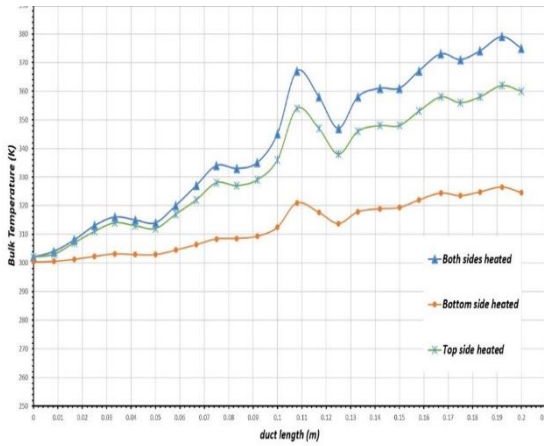

Figure 5. The effect of duct length on bulk temperature.

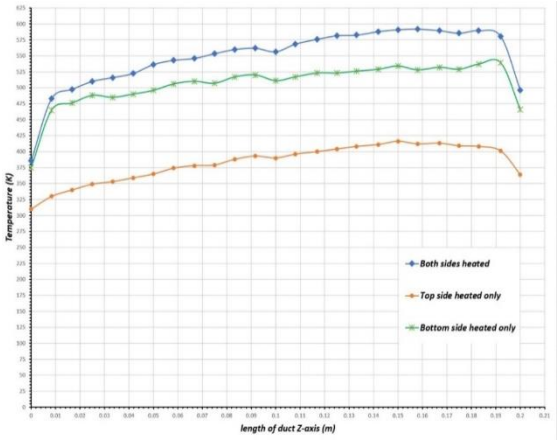

Figure 6. Comparisons of temperature distribution for each heated surface.

The values of temperature difference in the equation illustrate Nusselt number behavior, which is inversely proportional to the temperature difference and is illustrated in Fig. 7.

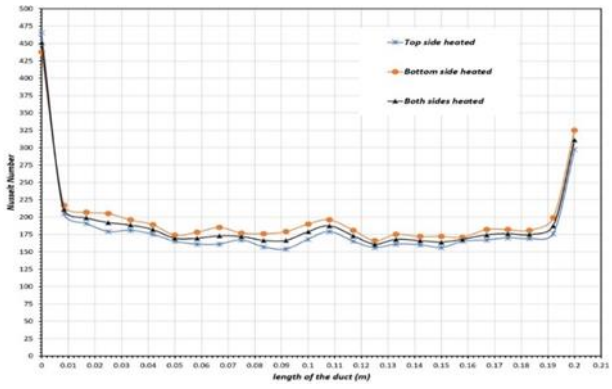

Figure 7. Variations of Nusselt number along the length of the duct

Figure 8 shows the comparison between the heating process of the upper and lower walls of the duct and the effect of the friction factors, the length of the duct, and several cross-sections along its length. Relationship between the abovementioned factors has clarified that the value of friction factor increased for each cross section along the length of the duct in which the velocity of close surface gradually decreasing due to the increasing in the resistance of the

surface wall so that the value of friction factors on the surface increase. It has noted that the velocity values gradually increased and the friction factor decreased as getting closer to the center of the stream and duct length as shown in Fig. 9.

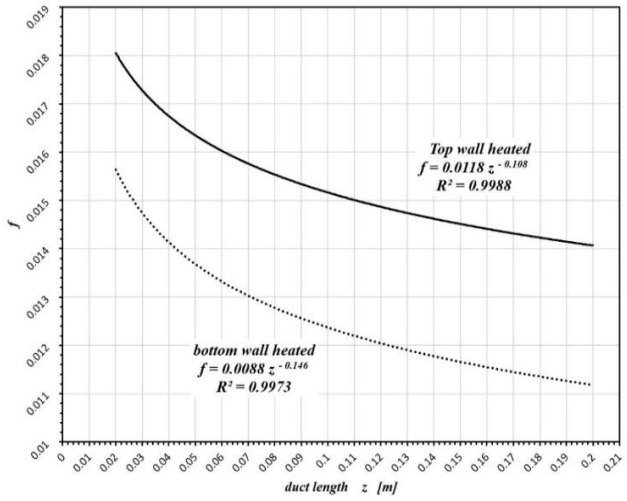

Figure 8. Friction factor comparison of top and bottom walls effect on the duct length.

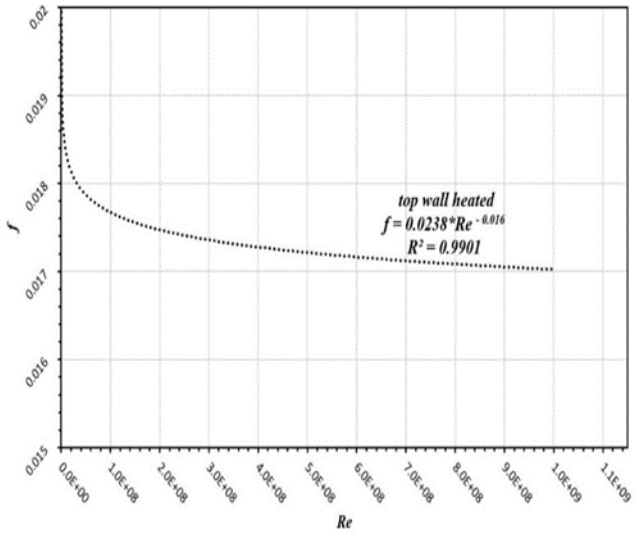

Figure 9. The friction factor of top wall heated effect on the Reynolds number.

CONCLUSIONS

Turbulent airflow has heated with one or more sides for the horizontal trapezoidal cross-sectional area which has dealt through the present research, a conclusion has drawn and represented in the following points:

1. The heating of the surface from the side accelerate the speed distribution of the adjacent layers.
2. Air and surface temperature distribution increase gradually along the course due to thermal heating.
3. The value of the Nusselt number decreases gradually along the course of the stream due to the increasing in the difference between the surface and fluid temperature in each section along the stream.
4. Fraction Factor decreases along the course due to the effect of the thickness of rounded-surface layer, the high velocity used in airflow calculations, in which it decreases to its lowest value at the center of the passage section.

5. When observing the temperature distribution of the heated air in fig 3, instability of the air temperature has noticed, because the properties used in the numerical analysis which represent the study are a function of temperature, which affects its distribution.

REFERENCES

[1] J.H. Lienha , "A heat transfer textbook", Courier Dover Publications, 2019.

[2] S. Eiamsa-ard and W. Changcharoe, "Flow structure and heat transfer in a square duct fitted with dual/quadruple twisted-tapes: Influence of tape configuration", J. Mech. Sci. Technol., vol. 29, No. 8, Pp. 3501–3518, 2015.

[3] P. Samruaisin, W. Changcharoen, C. Thianpong, V. Chuwattanakul, M. Pimsarn, and S. Eiamsa-ard, "Influence of regularly spaced quadruple twisted tape elements on thermal enhancement characteristics", Chem. Eng. Process. Intensif., Vol. 128, Pp. 114–123, 2018.

[4] A. Saysroy and S. Eiamsa-Ar , "Enhancing convective heat transfer in laminar and turbulent flow regions using multi-channel twisted tape inserts", Int. J. Therm. Sci., Vol. 121, Pp. 55–74, 2017.

[5] A. Eltaweel, A. Baobeid, B. Tompkins, and I. Hassa , "Numerical investigation of heat transfer characteristics of a novel wavy-tapered microchannel heat sink", in ASME 2016 Heat Transfer Summer Conference collocated with the ASME 2016 Fluids Engineering Division Summer Meeting and the ASME 2016 14th International Conference on Nanochannels, Microchannels, and Minichannels, 2016.

[6] S. Amirahmadi, S. Rashidi, and J.A. Esfahani, "Minimization of exergy losses in a trapezoidal duct with turbulator, roughness and beveled corners," Appl. Therm. Eng., Vol. 107, Pp. 533–543, 2016.

[7] L.I.U. Haiyong, H. Qiang, L.I.U. Songling, and L.I.U. Cunliang, "Flow field investigation in a trapezoidal duct with swirl flow induced by impingement jets," Chinese J. Aeronaut., Vol. 24, No. 1, Pp. 8–17, 2011.

[8] X. Zhang, Y. Wang, R. Jia, and R. Wan , "Investigation on heat transfer and flow characteristics of heat exchangers with different trapezoidal ducts," Int. J. Heat Mass Transf., Vol. 110, Pp. 863–872, 2017.

[9] P. Gogoi, M.K. Triveni, and R. Panu, "Numerical investigation of 3D turbulent forced convective heat transfer and friction characteristics of a square duct," Int. J. HEAT Technol., Vol. 35, No. 4, Pp. 919–932, 2017.

[10] D. Sharma, P.P. Singh, and H. Garg, "Comparative study of rectangular and trapezoidal microchannels using water and liquid metal," Procedia Eng., Vol. 51, Pp. 791–796, 2013.

[11] J.P. McHale and S.V. Garimella, "Heat transfer in trapezoidal microchannels of various aspect ratios," Int. J. Heat Mass Transf., Vol. 53, No. 1–3, Pp. 365–375, 2010.